Site-Dependent Coordination Bonding in Self-Assembled Metal−Organic Networks

N. Henningsen,[†] R. Rurali,[‡] C. Limbach,[†] R. Drost,[†] J. I. Pascual,[§] and K. J. Franke*[,§]
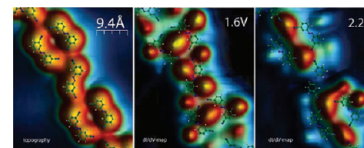
[†]Institut für Experimentalphysik, Freie Universität Berlin, Arnimallee 14, 14195 Berlin, Germany,
[‡]Institut de Ciència de Materials de Barcelona (ICMAB−CSIC), Campus de Bellaterra, 08193 Bellaterra (Barcelona), Spain, and [§]Institut für Experimentalphysik and Center for Supramolecular Interactions (CSI Berlin), Freie Universität Berlin, Arnimallee 14, 14195 Berlin, Germany

ABSTRACT The combination of organic linkers with metal atoms on top of inorganic substrates offers promising perspectives for functional electronic and magnetic nanoscale devices. Typically, coordination bonds between electron-rich end groups and transition-metal atoms lead to the self-assembly of metal−organic nanostructures, whose shape and electronic and magnetic properties crucially depend on the type of ligand. Here, we report on the site-selective bonding properties of Co atoms to the dichotomic dicyanoazobenzene molecule with its carbonitrile and diazo N-based moieties as possible ligands. Using low-temperature scanning tunneling microscopy (STM) and spectroscopy measurements, we resolve the formation of self-assembled metal−organic motifs. Cobalt atoms exhibit a clear spectroscopic fingerprint dependent on the different coordination site, which is further used to map their position, otherwise not clearly visible in the topographic STM images. Density functional theory corroborates the observed bonding patterns and evidences their coordinative nature.

SECTION Surfaces, Interfaces, Catalysis

The design and construction of supramolecular architectures and their use in devices is a fascinating perspective. In particular, the functionalization of surfaces by self-assembly comprises the possibility to create regular templates for selective adsorption,[1−3] controlling surface chemical reactions at well-defined reaction centers,[4,5] confining and tuning electronic states,[6−9] and creating magnetically coupled nanostructures.[10] The latter is especially appealing as one may envision the switching of spin states and controlling magnetic coupling within the layer by, for example, tuning chemical interactions.[11−13] A standard approach toward magnetic molecular lattices is monolayers of organic macrocycles with magnetic metal cores[14−20] grown on inorganic surfaces. Alternatively, recent studies have demonstrated that codeposition of transition-metal atoms with organic linkers leads to the formation of extended metal−organic networks stabilized by lateral atom-linker interactions.[21,22] This method offers the flexibility of using basic molecular building blocks and a cementing metal atom to construct extended coordination networks.

Beyond empirical approaches, current efforts are directed to understanding the coordination bond when confined to a two-dimensional plane, in which the interaction between the atoms and the organic ligands is expected to be influenced by the presence of the substrate.[23,24] This is particularly relevant when addressing the magnetic state of the metal centers because it can be quenched or altered substantially.[10,25] Similar to three-dimensional coordination chemistry, many of the

ligands used are based on nitrogen heteroatoms as the active donor, which are prone to coordinate to transition-metal atoms via their lone-pair electrons.[26] Previous studies have shown that transition-metal atoms bind to N sites of organic linkers, steering the formation of extended motifs, in which the metal center acts as a cementing node with a well-defined symmetry.[21−23,27] A recent study has shown that metal−ligand interactions rely on σ bonds with N lone-pair electrons.[28] The strength of this bond is expected to critically depend on the specific hybridization of the N atom within the organic linker.[26,29]

The purpose of the present study is to selectively probe the different character of the coordination bond of a transition-metal atom, cobalt, to N atoms with different chemical surroundings. We use low-temperature scanning tunneling spectroscopy (STS) to identify spectral (chemical) fingerprints associated with Co atoms bonded to N sites of an organic molecule. As an organic component, we use *trans*-dimetacyanoazobenzene (DMC)[30] because it holds four N active sites with either sp (carbonitrile) or sp^2 (diazo) character. Supported by model density functional theory (DFT) calculations, we find that cobalt atoms present a site-specific chemical signal in the spectra due to the different chemical character and symmetry of sp and sp^2 nitrogen sites. Spatial mapping of the spectroscopic signal
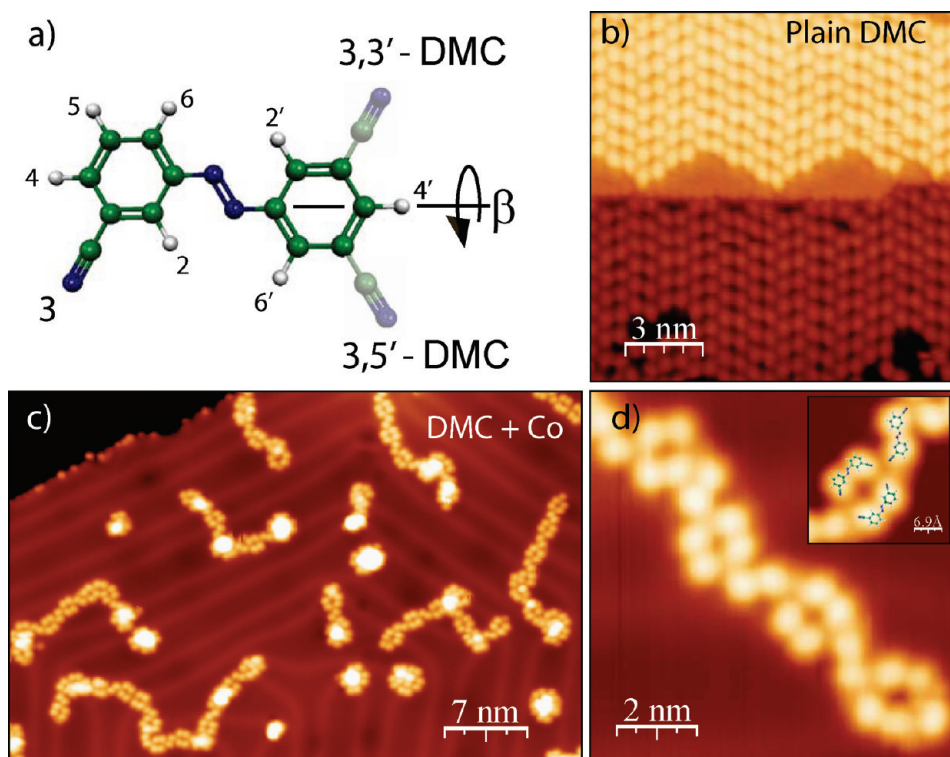
Figure 1. (a) Molecular structure of the dicyanoazobenzene (DMC) molecule indicating the rotational axis β around which the rotation of a phenyl ring results in the 3,3′ and 3,5′ conformation. (b) STM image of plain DMC ($U = 1.9\,\text{V}, I = 150\,\text{pA}$) and (c) that codeposited with cobalt atoms on a Au(111) surface. In (c), clusters of Co and chain structures of the molecular species can be observed ($U = 0.33\,\text{V}, I = 100\,\text{pA}$). (d) Close-up view of a DMC−Co chain. The inset shows the three-fold-symmetric Co site ($U = 0.3\,\text{V}, I = 55\,\text{pA}$).[40]

allows us to localize within the molecular backbone the bonding site of each Co atom depending on its coordination state.

DMC is composed of an azobenzene skeleton with two carbonitrile terminations in meta sites (Figure 1a). Although being a prototype molecular switch, only the trans isomers are stable on the gold surface.[31] They exhibit two energetically similar rotamer configurations described by rotations around the β axis (Figure 1a). When DMC is deposited on a clean Au(111) surface (see Experimental Methods section), compact and ordered two-dimensional domains, as shown in Figure 1b, are observed using scanning tunneling microscopy (STM) at low temperature (5 K). *trans*-DMC is imaged by the STM as a double lobe structure, each lobe corresponding to a cyano-phenyl moiety. The two rotamers can be distinguished by a slight lobe asymmetry in the STM images,[31] indicating the position of the cyano groups in either 3 or 5 meta sites (described in Figure 1a).

When, instead, a submonolayer amount of cobalt atoms is deposited on the Au(111) surface previous to DMC adsorption (see Experimental Methods section) chain structures are ubiquitously observed (Figure 1c,d), thus revealing the active role of this metal to steer a different type of molecular ordering. The chains appear, in general, bonded to and connecting sporadic cobalt clusters, remanents of the initial amount deposited. As in previous works on similar motifs,[23,32] we interpret these new string structures appearing exclusively on a cobalt-prepared surface as a clear expression of a metal−organic network created by the incorporation of single

cobalt atoms extracted from the codeposited clusters as cementing objects.

The string-like features exhibit an intrinsically disordered structure characteristic of the assembly of molecules with internal degrees of freedom.[32,33] However, we can identify a repeated pattern composed of three (two 3,5′- and one 3,3′-) DMC molecules pointing their cyano terminations to a three-fold bonding node (Figure 1d). This three-fold bonding scheme is highly unlikely for the bare electrophilic nitro terminations, unless they appear coordinated to a Co atom. Lone-pair electrons of nitrile moieties are known to be active to bond to transition-metal atoms via σ dative bonds with some amount of π back donation.[29] Indeed, similar three-fold motifs as those reported here were found in related nitrile-based species,[23,32] based on which we assign the chain structures to the presence of a cementing cobalt atom.

Apart from the cyano groups, DMC has additional N sites which might bond to codeposited cobalt atoms, the diazo bridge connecting both cyanophenyls. These predominantly sp^2 hybridized sites expose the nitrogen lone-pair electrons laterally outward, also acting as active sites for the bonding to transition metals, as has been found, for example, in the bonding of DMC to copper surfaces.[34] It is then expected that these sites may also interact with Co atoms.

Co adatoms are not visible in the STM images at low bias.[28] However, their existence can be demonstrated by means of tunneling spectroscopy. Figure 2b compares the differential conductance (dI/dV) spectra acquired on plain DMC islands
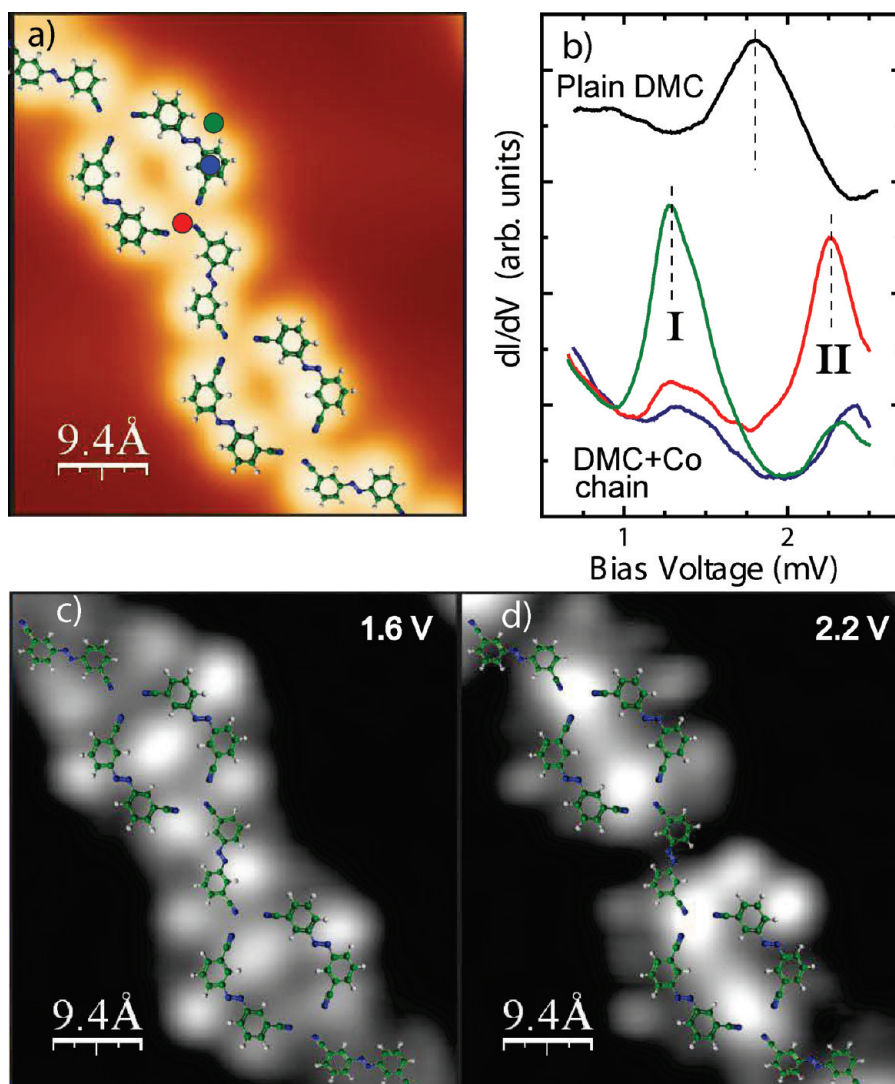
Figure 2. (a) Topographic STM image of a DMC−Co chain ($U = 0.9$ V, $I = 79$ pA). (b) Differential conductance (dI/dV) spectra acquired with a closed feedback loop (70 pA) at different locations on the DMC−Co chains as indicated in the STM image. The reference spectrum of plain DMC has been recorded on a phenyl ring of a molecule embedded in a pure DMC island. (c,d) Corresponding differential conductance maps at the energies of the resonances at the diazo and cyano Co sites, that is, at 1.6 and 2.2 V, respectively ($I = 79$ pA). Below 1 V, dI/dV maps solely show the shape of the DMC molecules. The strong energy dependence of the appearance of localized resonances next to the molecules is a clear fingerprint of the Co derived resonances and precludes significant topographic contributions to the dI/dV maps.[41]

on Au(111) and on different sites of the trimeric DMC + Co motifs. A clear resonance peak at +1.8 V (associated with an empty molecular state) in the reference spectrum on the plain DMC island is missing in the spectra on the cobalt− DMC chains. Instead, the latter shows pronounced unoccupied resonances localized at the cyano (peak II) and close to the diazo sites (peak I), where, according to the arguments above, cobalt atoms are expected. On trigonal cyano sites, the peak lies at 2.3 eV, whereas on the diazo sites, the resonance is observed at 1.3 eV. These spectroscopic fingerprints, not present on the plain species, further support the presence of the anticipated Co atoms. The different resonance energy depending on the specific N site reflects the different bonding character of the cobalt atoms and represents a chemical fingerprint of their bonding state with the organic linkers.

The localization of the resonances on cobalt atoms within the molecular chains is further revealed by spatially mapping the dI/dV signal. By setting the sample bias to the value of each resonance state from Figure 2, we can selectively image the cobalt atoms in their specific chemical state within the metal−organic structures. The maps in Figure 2c and d show that at 2.2 V, the maximum dI/dV signal is localized at the trigonal sites of the chain, whereas the 1.3 V resonance appears localized at points in the proximity of the diazo bridge and, in a few occasions, at several other neighboring sites. In general, the dI/dV maps show that most of the molecular N sites are occupied by cobalt atoms. Furthermore, we see that the atomic features resolved at each bias are hardly seen at the other, thus demonstrating the concept of selectively imaging metal atoms according to their bonding state.
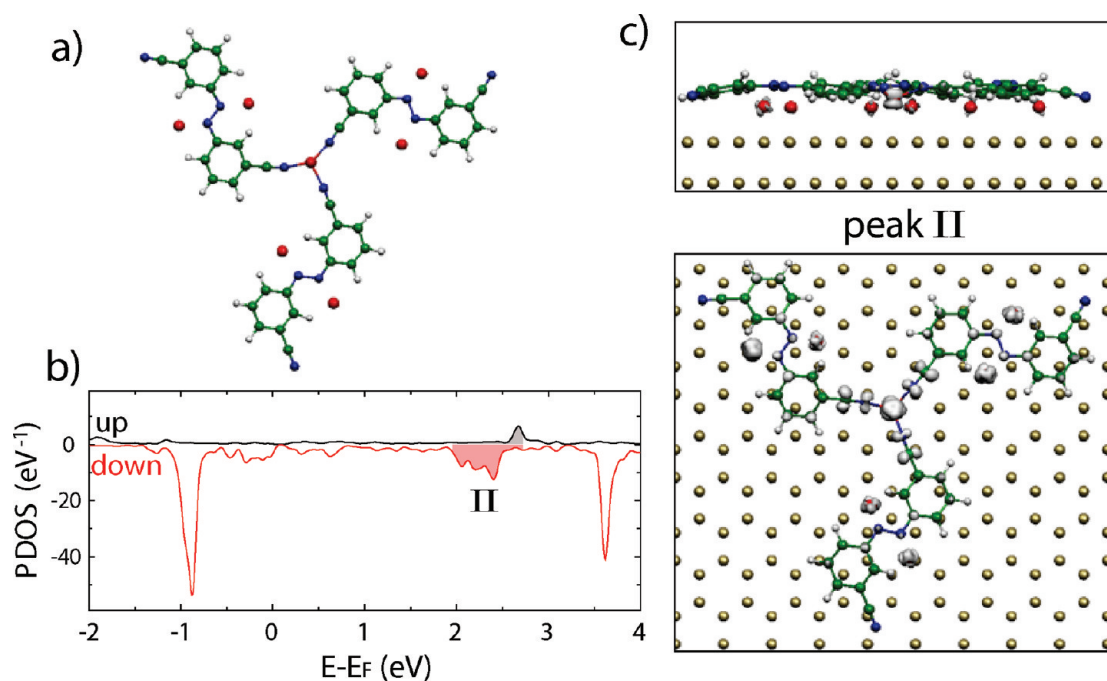
Figure 3. (a) Top view of the optimized DMC + Co stand-alone structure. (b) Spin-polarized density of states projected on orbitals of trigonal Co atoms for the structure of (a) relaxed on a Au(111) bilayer. The sharp states at ∼−0.9 and ∼+3.6 eV and those at ∼−2.6 eV (not shown in Figure 3b) collect most of the weight on Co d_{xz}, d_{yz}, d_{xy}, and $d_{x^2-y^2}$ orbitals. Their sharpness and energy degeneracy suggest a weak distortion by the surface and by the in-plane organic linkers. (c) Constant charge density isosurface of states within a 0.7 eV energy window around 2.3 eV (shadowed in (b)). The accumulation of states at the Co-3 × CN motif is in qualitative agreement with the sites where experimental peak II appears localized.

In order to gain further insight into the origin of the resonances in terms of their bonding to the organic skeleton, we have performed electronic structure calculations within DFT (see Theoretical Methods section). Our approach is to first simulate the structure of a free layer composed of three DMC molecules, six Co atoms close to the diazo bridge, and one atom at the three-fold node connecting three molecules via their CN termination (see Figure 3a). In this way, it is possible to tackle various problems such as the bonding of Co atoms to different parts of the molecule and their magnetic interaction. The relaxed structure clearly finds a tendency of Co atoms to form chemical bonds to N atoms of the organic backbone. In this model structure, the Co−N bond distance amounts to ∼1.94 and ∼1.84 Å, and the bonding energies are 0.86 and 8.23 eV per cobalt atom bonded to diazo and cyano sites, respectively. The bond to the cyano termination is significantly stronger (2.74 eV per bond), this being the main interaction leading to the extraction of Co atoms from the predeposited clusters and the stabilization of the metal−organic structures. The electronic structure of the free layer already reproduces different peaks in the density of states associated with the two different types of coordinated Co atoms.

In a second step, the stand-alone molecular layer of Figure 3a was placed on top of an unreconstructed Au(111) bilayer, and subsequently, its atomic structure was relaxed (see Theoretical Methods section). The presence of the surface induces small changes on the structure of the metal−organic motif. The adsorption is governed by the interaction of Co atoms with the Au surface, anchoring the molecular backbones

via their N sites. In this sense, the system does not behave as a weakly bound layer. The molecular layer finds a minimum-energy configuration at an average distance of 3 Å, but the Co atoms are further attracted toward the surface, lying at 2 and 2.2 Å for those ions sitting close to the diazo bridge and at the CN termination sites, respectively.[35] The higher position of the trigonal Co atoms reflects a stronger bond with the molecular end groups.

To track the origin of the two resonances observed in the STS spectra, we project the density of states (DOS) of the whole (molecule + surface) system on the atomic orbitals of cobalt atoms bonding to either trigonal CN (Figure 3b) or diazo (Figure 4a) sites. The projected DOS (PDOS) on cobalt atoms at trigonal nodes reproduces sharp features at −0.9 and 3.6 eV (and at −2.6 eV, not shown in the figure), originating essentially from cobalt d states. Splitting the PDOS plot in terms of individual Co d orbitals shows that all of these sharp peaks have essentially d_{xz}, d_{yz} and d_{xy}, $d_{x^2-y^2}$ character, while the d_{z^2} orbital is strongly broadened as a consequence of its interaction with the underlying surface. A fingerprint of the bond to CN moieties can be found in the energy region of the experimental dI/dV resonances. At around ∼2.3 eV, the PDOS shows a broader accumulation of peaks (shaded region in Figure 3b). Constant DOS surfaces associated to wave functions in this energy window (±0.375 eV at around 2.3 eV) show that these states are localized at the trigonal cobalt sites. Furthermore, the DOS isosurfaces spread into the cyano terminations with the shape of the N≡C π^* orbitals (Figure 3c), reflecting the coordinative nature of the bond. The energy
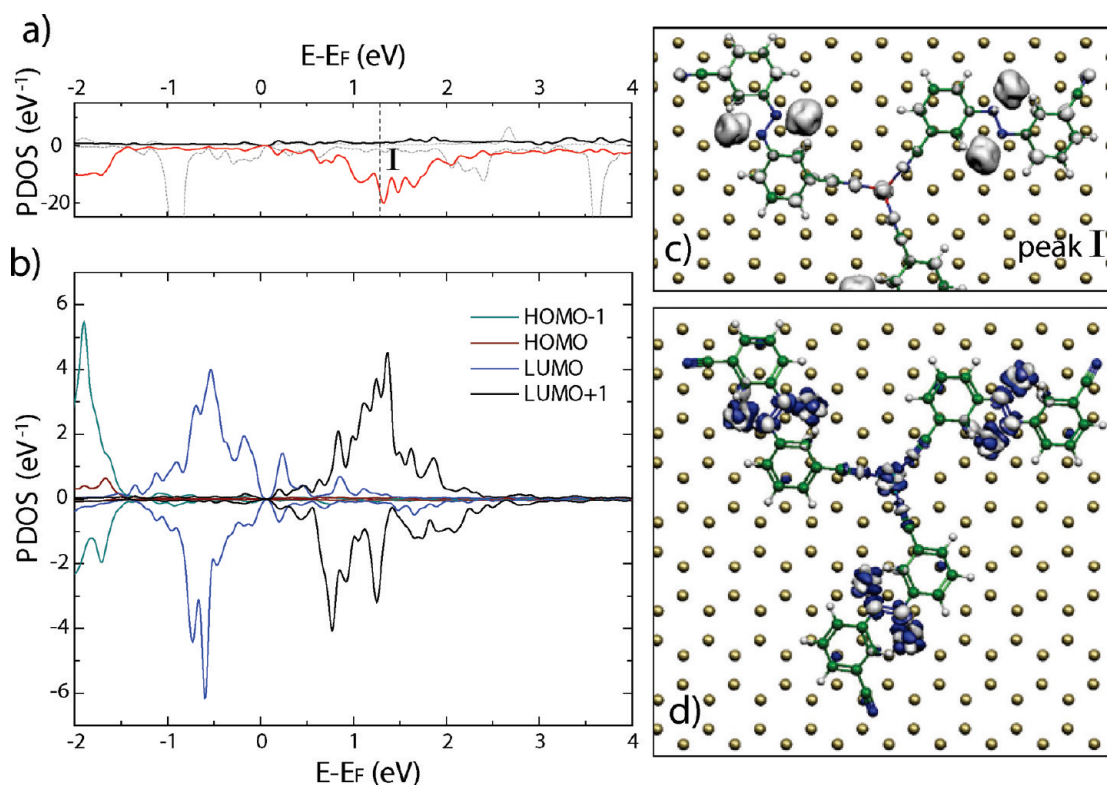
Figure 4. Spin-polarized density of states projected on (a) orbitals of diazo-bonded Co atoms (black: spin up; red: spin down; gray lines reproduce the PDOS from Figure 3b, for comparison) and (b) DMC molecular orbitals for the structure shown in (a) relaxed on a Au(111) bilayer. In (b), some spin structure emerges in the states derived from molecular orbitals due to their interaction with the neighboring Co atoms. (c) Constant charge density isosurface of states within a 0.7 eV energy window around 1.3 eV. The accumulation of states at the diazo Co−N sites agrees with the spatial localization of the peak I observed in Figure 2. (d) Induced charge density isosurfaces (see Theoretical Methods section). Both types of bonded Co atoms induced substantial reorganization of electron density at the neighboring N sites, making it possible to recognize the spatial shape of lone pair orbitals at the diazo sites.

and space localization of these cobalt states lies in qualitative agreement with the peak II in the dI/dV spectra, thus confirming its assignment to resonances of the Co-3 × CN coordinated moiety.

The electronic states derived from the Co atoms at the diazo site appear more broadened in the corresponding PDOS (Figure 4a), in agreement with their lower symmetry and the stronger interaction with the metal substrate. A broad accumulation of states nucleates at around 1.5 eV, where peak I was found in the experiment, but the reduced symmetry of these sites hinders a clear identification of the peak origin in terms of Co d orbitals. Instead, the calculations suggest that the dI/dV resonance has a marked molecular character. Projection of the total DOS onto molecular states of the free DMC molecule (Figure 4b) finds states arising from the LUMO+1 molecular orbital at a similar energy value (∼1.5 eV), whereas the DMC LUMO resonance is occupied as a result of charge transfer.[34] The corresponding DOS isosurface, obtained by integrating now wave functions in a ±0.375 eV energy window around 1.3 eV, is more localized around the cobalt atoms close to diazo sites (Figure 4c), coinciding with the experimental dI/dV peak I, observed at 1.3 eV and centered at these sites. The existence of a chemical bond between cobalt atoms and diazo N sites is evidenced by accounting the charge redistribution due to the presence of

the metal atom. Figure 4d maps the difference in total charge density (i.e., the induced charge density) in the system arising upon removal of all of the cobalt atoms from the relaxed atomic structure (see Experimental Methods section). The induced charge is localized at both the diazo and the cyano N sites, showing the shape of the lone-pair and π orbitals, respectively. In both cases, a chemical bond with the metal atoms can be concluded.

Our conclusions on the different strength of the interaction with the substrate experienced by the diazo and trigonal Co atoms is consistent with the variation of their atomic charge. Within the qualitative approach of our model calculations, a Mulliken population analysis shows a systematic loss of 0.3 e from the diazo Co, while the trigonal Co, whose interaction with the substrate is weaker, maintains the nominal charge of the isolated atom. The total spin polarization, that is, the difference between the spin up and spin down population, is entirely carried by the d states of the Co atoms (as expected and as happens for the free Co atom) and amounts to ∼20 μ_B (our computational supercell contains seven Co atoms). Both types of cobalt atoms display a similar behavior; the diazo cobalt atoms keep the magnetization state of the isolated species, ∼3 μ_B per atom (hence, spin 3/2), whereas the atoms sitting at the trigonal CN sites exhibit a magnetization state of ∼2.5 μ_B, also close to the nominal value of the free atom.

The interaction of cobalt atoms with N lone-pair electrons depends strongly on the type of organic ligand. Using tunneling spectroscopy, we map the different bonding fingerprints in dI/dV spectra at their corresponding energies and thus also detect Co atoms which are hardly visible in the topographic STM images. DFT calculations corroborate the interpretation of mapping different bonding schemes and explain the bond character on the basis of chemical interactions between Co and N atoms. In particular, a clear-cut fingerprint of coordination bonding on a surface is given at cyano-ligated Co atoms. The cobalt atoms remain close to a zero oxidation state, maintaining magnetic moments close to the nominal values of the free atom.

EXPERIMENTAL METHODS

Our experiments were carried out in a custom-built low-temperature STM under ultrahigh vacuum conditions, at a temperature of 5 K. Atomically clean (111)-oriented Au single crystals, prepared using standard sputtering−annealing methods, were used as the substrate. To grow the metal−organic structures, a submonolayer amount of cobalt atoms was first deposited on the clean gold surface using an electron beam evaporator. At room temperature, Co adatoms nucleated on the Au(111) surface in small clusters pinned at the corners of the herringbone reconstruction.[36] Subsequent deposition of DMC molecules using a Knudsen Cell and annealing of the mixed system to 330 K led to the thermal activation of the organic−metal linkage.

THEORETICAL METHODS

The electronic structure calculations were performed within DFT as implemented in the Siesta package.[37] We used a double-ζ polarized basis set for the valence electron, norm-conserving pseudopotentials of the Troullier−Martins type to model the core electron and the General Gradient Approximation (GGA)[38] for the exchange−correlation energy functional. The molecular layer of Figure 3a was placed on top of an unreconstructed Au(111) bilayer, and subsequently, its atomic structure was relaxed, while maintaining the gold atoms fixed. A vacuum buffer of ± 35 Å was used to minimize the interaction of the adsorbate/substrate slab from its periodic images. We sampled the Brillouin zone with the Γ point. This model approach qualitatively captures relaxed structures, charge transfer with the molecular adsorbate, and a description of the electronic structure, as has been previously shown on similar systems,[23,28,35] while keeping the computational effort within reasonable capabilities.

The PDOS on cobalt and molecular orbitals has been done following the method described in ref 39. The induced charge density plots have been obtained by accounting for the difference between the total charge of the complete system ($3 \times$ DMC + $7 \times$ Co + Au) minus the total charge of the $3 \times$ DMC + Au layer and the isolated $7 \times$ Co atoms, all of them fixed at their originally relaxed positions. The robustness of the obtained electronic structure upon small geometrical changes caused by, for example, van der Waals interactions (neglected in this study) or the poor description of the Au surface due to computational limitations has been tested by comparing with results of the frozen molecular layer for different distances (± 0.2 Å) to the metal surface.

AUTHOR INFORMATION

Corresponding Author:
*To whom correspondence should be addressed. E-mail: franke@physik.fu-berlin.de.

REFERENCES

(1) Theobald, J. A.; Oxtoby, N. S.; Phillips, M. A.; Champness, N. R.; Beton, P. H. Controlling Molecular Deposition and Layer Structure with Supramolecular Surface Assemblies. *Nature* **2003,** *424,* 1029–1031.

(2) Corso, M.; Auwärter, W.; Muntwiler, M.; Tamai, A.; Greber, T.; Osterwalder, J. Boron Nitride Nanomesh. *Science* **2004,** *303,* 217–220.

(3) Stepanow, S.; Lingenfelder, M.; Dmitriev, A.; Spillmann, H.; Delvigne, E.; Lin, N.; Deng, X.; Cai, X.; Barth, J. V.; Kern, K. Steering Molecular Organization and Host−Guest Interactions Using Two-Dimensional Nanoporous Coordination Systems. *Nat. Mater.* **2004,** *3,* 229–232.

(4) Davis, M. E. Ordered Porous Materials for Emerging Applications. *Nature* **2002,** *417,* 813–821.

(5) Gopakumar, T. G.; Neel, N.; Kröger, J.; Berndt, R. Spatial Modulation of d States in a Nanoscale Co Island. *Chem. Phys. Lett.* **2009,** *484,* 59–63.

(6) Pennec, Y.; Auwärter, W.; Schiffrin, A.; Weber-Bargioni, A.; Barth, J. V. Supramolecular Gratings for Tuneable Confinement of Electrons on Metal Surfaces. *Nat. Nanotechnol.* **2007,** *2,* 99–103.

(7) Gonzalez-Lakunza, N.; Fernandez-Torrente, I.; Franke, K. J.; Lorente, N.; Arnau, A.; Pascual, J. I. Formation of Dispersive Hybrid Bands at an Organic−Metal Interface. *Phys. Rev. Lett.* **2008,** *100,* 156805.

(8) Lobo-Checa, J.; Matena, M.; Müller, K.; Dil, J. H.; Meier, F.; Gade, L. H.; Jung, T. A.; Stöhr, M. Band Formation from Coupled Quantum Dots Formed by a Nanoporous Network on a Copper Surface. *Science* **2009,** *325,* 300–303.

(9) Klappenberger, F.; Kühne, D.; Krenner, W.; Silanes, I.; Arnau, A.; Garcia de Abajo, F. J.; Klyatskaya, S.; Ruben, M.; Barth, J. V. Dichotomous Array of Chiral Quantum Corrals by a Self-Assembled Nanoporous Kagome Network. *Nano Lett* **2009,** *9,* 3509–3514.

(10) Seitsonen, A. P.; Lingenfelder, M.; Spillmann, H.; Dmitriev, A.; Stepanow, S.; Lin, N.; Kern, K.; Barth, J. V. Density Functional Theory Analysis of Carboxylate-Bridged Diiron Units in Two-Dimensional Metal−Organic Grids. *J. Am. Chem. Soc.* **2006,** *128,* 5634–5635.

(11) Wende, H.; Bernien, M.; Luo, J.; Sorg, C.; Popandian, N.; Kurde, J.; Miguel, J.; Piantek, M.; Xu., X.; Eckhold, Ph.; et al. Substrate-Induced Magnetic Ordering and Switching of Iron Porphyrin Molecules. *Nat. Mater.* **2007,** *6,* 516–520.

(12) Wegner, D.; Yamachika, R.; Zhang, X.; Wang, Y.; Baruah, T.; Pederson, M. R.; Bartlett, B. M.; Long, J. R.; Crommie, M. F. Tuning Molecule-Mediated Spin Coupling in Bottom-Up-Fabricated

Vanadium-tetracyanoethylene Nanostructures. *Phys. Rev. Lett.* **2009,** *103,* 087205.

(13) Liljeroth, P.; Swart, I.; Paavilainen, S.; Repp, J.; Meyer, G. Single-Molecule Synthesis and Characterization of Metal−Ligand Complexes by Low-Temperature STM. *Nano Lett.* **2010,** *10,* 2475–2479.

(14) Zhao, A.; Li, Q.; Chen, L.; Xiang, H.; Wang, W.; Pan, S.; Wang, B.; Xiao, X.; Yang, J.; Hou, J. G.; Zhu, Q. Controlling the Kondo Effect of an Adsorbed Magnetic Ion Through Its Chemical Bonding. *Science* **2005,** *309,* 1542–1544.

(15) Iancu, V.; Deshpande, A.; Hla, S.-W. Manipulation of the Kondo Effect via Two-Dimensional Molecular Assembly. *Phys. Rev. Lett.* **2006,** *97,* 266603.

(16) Fu, Y.-S.; Ji, S.-H.; Chen, X.; Ma, X.-C.; Wu, R.; Wang, C.-C.; Duan, W.-H.; Qiu, X.-H.; Sun, B.; Zhang, P.; et al. Manipulating the Kondo Resonance through Quantum Size Effects. *Phys. Rev. Lett.* **2007,** *99,* 256601.

(17) Iacovita, C.; Rastei, M. V.; Heinrich, B. W.; Brumme, T.; Kortus, J.; Limot, L.; Bucher, J. P. Visualizing the Spin of Individual Cobalt-Phthalocyanine Molecules. *Phys. Rev. Lett.* **2008,** *101,* 116602.

(18) Tsukahara, N.; Noto, K.; Ohara, M.; Shiraki, S.; Takagi, N.; Takata, Y.; Miyawaki, J.; Taguchi, M.; Chainani, A.; Shin, S.; Kawai, M. Adsorption-Induced Switching of Magnetic Anisotropy in a Single Iron(II) Phthalocyanine Molecule on an Oxidized Cu(110) Surface. *Phys. Rev. Lett.* **2009,** *102,* 167203.

(19) Brede, J.; Atodiresei, N.; Kuck, S.; Lazić, P.; Caciuc, V.; Morikawa, Y.; Hoffmann, G.; Blügel, S.; Wiesendanger, R. Spin- and Energy-Dependent Tunneling through a Single Molecule with Intramolecular Spatial Resolution. *Phys. Rev. Lett.* **2010,** *105,* 047204.

(20) Stepanow, S.; Mugarza, A.; Ceballos, G.; Moras, P.; Cezar, J. C.; Carbone, C.; Gambardella, P. Giant Spin and Orbital Moment Anisotropies of a Cu-phthalocyanine Monolayer. *Phys. Rev. B* **2010,** *82,* 014405.

(21) Stepanow, S.; Lin, N.; Barth., J. V. Modular Assembly of Low-Dimensional Coordination Architectures on Metal Surfaces. *J. Phys.: Condens. Matter* **2008,** *20,* 184002.

(22) Barth, J. V. Fresh Perspectives for Surface Coordination Chemistry. *Surf. Sci.* **2009,** *603,* 1533–1541.

(23) Schlickum, U.; Decker, R.; Klappenberger, F.; Zoppellaro, G.; Klyatskaya, S.; Ruben, M.; Silanes, I.; Arnau, A.; Kern, K.; Brune, H.; Barth, J. V. Metal−Organic Honeycomb Nanomeshes with Tunable Cavity Size. *Nano Lett.* **2007,** *7,* 3813–3817.

(24) Stepanow, S.; Lin, N.; Payer, D.; Schlickum, U.; Klappenberger, F.; Zoppellaro, G.; Ruben, M.; Brune, H.; Barth, J. V.; Kern, K. Surface-Assisted Assembly of 2D Metal−Organic Networks That Exhibit Unusual Threefold Coordination Symmetry. *Angew. Chem., Int. Ed.* **2007,** *46,* 710–713.

(25) Gambardella, P.; Stepanow, S.; Dmitriev, A.; Honolka, J.; de Groot, F. M. F.; Lingenfelder, M.; Gupta, S. S.; Sarma, D. D.; Bencok, P.; Stanescu, S.; et al. Supramolecular Control of the Magnetic Anisotropy in Two-Dimensional High-Spin Fe Arrays at a Metal Interface. *Nat. Mater.* **2009,** *8,* 189–193.

(26) Jean, Y. *Molecular Orbitals of Transition Metal Complexes*; Oxford University Press: New York, 2005.

(27) Pawin, G.; Wong, K. L.; Kim, D.-H.; Sun, D.; Bartel, L.; Hong, S.; Rahman, T. S.; Carp, R.; Marsella, M. A Surface Coordination Network based on Substrate-Derived Metal Adatoms with Local Charge Excess. *Angew. Chem.* **2008,** *47,* 8442–8445.

(28) Björk, J.; Matena, M.; Dyer, M. S.; Enache, M.; Lobo-Checa, J.; Gade, L. H.; Jung, T. A.; Stöhr, M.; Persson, M. STM Fingerprint of Molecule−Adatom Interactions in a Self-Assembled Metal−Organic Surface Coordination Network on Cu(111). *Phys. Chem. Chem. Phys.* **2010,** *12,* 8815–8821.

(29) Kuznetsov, M. L. Is the Charge on the Nitrile Carbon Atom a Driving Force of the Nucleophilic Addition to Coordinated Nitriles? *J. Mol. Struct.: THEOCHEM* **2004,** *674,* 33–42.

(30) Priewisch, B.; Rück-Braun, K. Efficient Preparation of Nitrosoarenes for the Synthesis of Azobenzenes. *J. Org. Chem.* **2005,** *70,* 2350.

(31) Henningsen, N.; Franke, K. J.; Torrente, I. F.; Schulze, G.; Priewisch, B.; Rück-Braun, K.; Dokic, J.; Klamroth, T.; Saalfrank, P.; Pascual, J. I. Inducing the Rotation of a Single Phenylene ring with Tunneling Electrons. *J. Phys. Chem. C* **2007,** *111,* 14853–14848.

(32) Marschall, M.; Reichert, J.; Weber-Bargioni, A.; Seufert, K.; Auwärter, W.; Klyatskaya, S.; Zoppellaro, G.; Ruben, M.; Barth, J. V. Random Two-Dimensional String Networks Based on Divergent Coordination Assembly. *Nat. Chem.* **2010,** *2,* 131–137.

(33) Henningsen, N.; Franke, K. J.; Schulze, G.; Fernandez-Torrente, I.; Priewisch, B.; Rück-Braun, K.; Pascual, J. I. Active Intramolecular Conformational Dynamics Controllingthe Assembly of Azobenzene Derivatives at Surfaces. *Chemphyschem* **2008,** *9,* 71–73.

(34) Henningsen, N.; Rurali, R.; Franke, K. J.; Fernández-Torrente, I.; Pascual, J. I. Trans to Cis Isomerization of an Azobenzene Derivative on a Cu(100) Surface. *Appl. Phys. A: Mater. Sci. Process.* **2008,** *93,* 241–246.

(35) Wang, W.; Hong, Y.; Shi, X.; Minot, C.; Van Hove, M. A.; Tang, B. Z.; Lin, N. Inspecting Metal-Coordination-Induced Perturbation of Molecular Ligand Orbitals at a Submolecular Resolution. *J. Phys. Chem. Lett.* **2010,** *1,* 2295–2298.

(36) Schouteden, K.; Lando, A.; Janssens, E.; Van Haesendonck, C.; Lievens, P. Morphology and Electron Confinement Properties of Co Clusters Deposited on Au(111). *New J. Phys.* **2008,** *10,* 083005.

(37) Soler, J. M.; Artacho, E.; Gale, J. D.; García, A.; Junquera, J.; Ordejón, P.; Sánchez-Portal, D. The SIESTA Method for Ab Initio Order-N Materials Simulation. *J. Phys.: Condens. Matter* **2002,** *14,* 2745.

(38) Perdew, J. P.; Burke, K.; Ernzerhof, M. Generalized Gradient Approximation Made Simple. *Phys. Rev. Lett.* **1996,** *77,* 3865–3868.

(39) Lorente, N.; Hedouin, M. F. G.; Palmer, R.; Persson, M. Chemisorption of Benzene and STM Dehydrogenation Products on Cu(100). *Phys. Rev. B* **2003,** *68,* 155401.

(40) Horcas, I.; Fernandez, R.; Gomez-Rodriguez, J.; Colchero, J.; Gomez-Herrero, J.; Baro, A. WSXM: A Software for Scanning Probe Microscopy and a Tool for Nanotechnology. *Rev. Sci. Instrum.* **2007,** *78,* 013705.

(41) Ziegler, M.; Néel, N.; Sperl, A.; Kröger, J.; Berndt, R. Local Density of States from Constant-Current Tunneling Spectra. *Phys. Rev. B* **2009,** *80,* 125402.